*Korean J. Chem. Eng.*, 39(7), 1936-1945 (2022)
DOI: 10.1007/s11814-022-1114-3

pISSN: 0256-1115
eISSN: 1975-7220

# Deep dechlorination of hydrocarbon oil by reactive adsorption on $TiO_2$-based metal oxides

**Hui Niu, Yuyu Feng, Jie Ding, Wei Zhang†, Chenxing Hu, Qingxiang Zhang, Chen Zhang†, and Cuiqing Li**

Beijing Key Laboratory of Fuels Cleaning and Advanced Catalytic Emission Reduction Technology, College of New Materials and Chemical Engineering, Beijing Institute of Petrochemical Technology, Beijing 102617, China
(*Received 22 September 2021 • Revised 28 February 2022 • Accepted 15 March 2022*)

**Abstract**−This study reports reactive adsorptive dechlorination of hydrocarbon oil over $TiO_2$-based metal oxides at the temperatures of 20-150 °C. $TiO_2$ and a series of $TiO_2$-$CeO_2$ were prepared by precipitation method and characterized by $N_2$ adsorption, XRD, FT-IR, pyridine-IR, $NH_3$-TPD and $CO_2$-TPD. The characterization results showed that both the acidity and basicity of the adsorbent had a significant impact on its dechlorination capacity. $TiO_2$-U precipitated by urea exhibited higher dechlorination capacity than $TiO_2$-A precipitated by ammonia due to the higher surface area, more acid and base amounts of the former. Among various $Ti_{(1-x)}Ce_xO_2$ (x=0.1, 0.3, 0.5, 0.7, 0.9, 1) oxides, $Ti_{0.7}Ce_{0.3}O_2$ and $Ti_{0.3}Ce_{0.7}O_2$ bimetallic oxides showed higher dechlorination capacity than $TiO_2$-U, and the chlorine removal over $Ti_{0.7}Ce_{0.3}O_2$ reached 82.8% after adsorption at 150 °C for 3 h. Mixing 5 wt% of alkali earth metal oxide into $Ti_{0.7}Ce_{0.3}O_2$ mechanically enhanced its dechlorination capacity, and the chlorine removal over $Ti_{0.7}Ce_{0.3}O_2$-BaO reached as high as 92.1%. The chlorine removal increased with increasing the adsorption temperature. Ion chromatography and GC-MS analysis revealed that organochlorine compound was converted into $Cl^-$ and its corresponding alcohol over the adsorbent at 150 °C. Finally, the mechanism of reactive adsorption dechlorination was proposed.

Keywords: Adsorptive Dechlorination, 1-Chlorooctane, Plastic Pyrolysis Oil, $TiO_2$-$CeO_2$, Hydrolysis

## INTRODUCTION

Deep dechlorination of hydrocarbon oil has become an increasingly important subject worldwide [1-3]. Organochlorine in crude oil and its distillates tends to be converted to HCl during oil processing, causing serious corrosion to the refining equipment and also poisoning catalysts for hydrofining and catalytic reforming [4]. Besides, pyrolysis recycling of plastic waste calls for dechlorination of plastic pyrolytic oil [5,6]. As plastic waste is not biodegradable, its disposal becomes a serious environmental issue. Converting plastic waste to high value-added hydrocarbon oil by pyrolysis has been recognized as a promising route for the recycling of plastic waste [7,8]. However, organochlorine compounds in plastic pyrolysis oil derived from polyvinyl chloride (PVC) seriously affect the downstream processing of plastic pyrolytic oil. Hence, it is highly essential to remove the organochlorine from various hydrocarbon oils.

Several dechlorination methods have been developed in recent years, including hydrodechlorination [9,10], catalytic dechlorination [11,12], adsorptive dechlorination [13,14], and dechlorination by nucleophilic substitution [15,16]. Hydrodechlorination is a widely studied dechlorination method, by which organochlorine is catalytically converted to HCl over a noble metal catalyst, e.g., supported Ag-Pd [9] and Pt-Pd [17] in the presence of hydrogen under high temperature and high pressure. Nevertheless, hydrodechlorination technology has not been applied in industry so far due to the inherent problem of severe operation condition, high cost, and poisoning of its catalyst by HCl [13]. In contrast to hydrodechlorination, adsorptive dechlorination, which employs porous materials to selectively adsorb organochlorine from hydrocarbon oil, has been considered as a very promising dechlorination approach due to mild operation condition and low cost. Zeolites [13,14,18] and metal oxides [19,20] are the most commonly used dechlorination adsorbents due to their high dechlorination capacity and good regenerability. Zhang et al. [13] prepared Zn/H$\beta$ adsorbent for dechlorination of the model naphtha at 25 °C, and found that 72.54% of organochlorine could be removed over Zn/H$\beta$ and the adsorbent still maintained good dechlorination performance after regeneration for five times. To improve the adsorptive dechlorination efficiency, some researchers investigated adsorption dechlorination at elevated temperature [1,21]. Ge et al. [18] studied dechlorination of reformate over Ce-Y zeolite in a tubular microreactor in a temperature range from 100 °C to 150 °C, and found that the chlorine removal sharply increased from ~20% to ~80% when the temperature was elevated from 100 °C to 150 °C. Jiang [20] carried out adsorptive dechlorination of chlorinated hydrocarbon over $Na_2CO_3$/$Al_2O_3$ or $CaCO_3$/$Al_2O_3$, and reported that the dechlorination rate of chlorobenzene reached 90% over $Na_2CO_3$/$Al_2O_3$ at 410 °C. Niu [1] investigated adsorptive dechlorination of hydrocarbon oil over porous oxides at different temperatures, and the results showed that the removal of 1-chlorooctane over $Al_2O_3$ sharply increased from ~5% at 20 °C to 99% at 150 °C. These findings strongly demonstrate that deep dechlorination could be achieved over metal oxides or zeolites at elevated temperatures. Nevertheless, the mechanism

†To whom correspondence should be addressed.
E-mail: wzhang@bipt.edu.cn, zhangc@bipt.edu.cn
Copyright by The Korean Institute of Chemical Engineers.

of dechlorination at elevated temperatures, as well as the roles of acid sites and basic sites of adsorbents in dechlorination, still remain unclear and need to be investigated and clarified. Moreover, the dechlorination performance of adsorbents needs to be further improved for industrial application.

The objective of this paper is to investigate the mechanism of dechlorination of hydrocarbon oil at elevated temperatures, the roles of acid sites and basic sites of adsorbents in dechlorination, as well as to develop adsorbents with high dechlorination capacity. Attributed to tunable surface area and pore size, controllable functionality and good chemical stability, $TiO_2$ has been widely used in adsorption and catalysis areas [22-24]. Moreover, coupling $CeO_2$ into $TiO_2$ will lead to an increase in its surface area and a change in its surface chemistry [25,26]. In this work, $TiO_2$ and a series of $TiO_2$-$CeO_2$ were prepared by precipitation method and used for adsorptive dechlorination of hydrocarbon oil under different temperatures. The adsorbents were characterized by $N_2$ adsorption, X-ray diffraction (XRD), Fourier transform infrared spectroscopy (FT-IR), temperature-programmed desorption of $NH_3$ ($NH_3$-TPD) and $CO_2$ ($CO_2$-TPD), and infrared spectroscopy of pyridine (pyridine-IR). The influences of precipitants, Ti/Ce molar ratio in $TiO_2$-$CeO_2$, and adsorption temperature on the dechlorination performance were investigated. Dechlorination capacity of $TiO_2$-$CeO_2$ for various organochlorine compounds and the regenerability of $TiO_2$-$CeO_2$ were studied. To improve the dechlorination performance of $TiO_2$-$CeO_2$, $TiO_2$-$CeO_2$ was mixed with various alkaline earth metal oxides mechanically and their dechlorination performance was also evaluated. The reaction products of 1-chlorooctane were identified by GC-MS and ion chromatography (IC), and the mechanism of reactive adsorption dechlorination was proposed.

## EXPERIMENTAL SECTION

### 1. Materials

1-Chlorooctane (99%), 1,2-dichlorobenzene (99%), dodecane (98%), $TiCl_4$ and BaO were supplied by Aladdin Reagent Co., Ltd. $(NH_2)_2Ce(NO_3)_6$ and urea was obtained from Tianjin Guangfu Science & Technology Development Co., Ltd., China. $CaCO_3$ and urea (99%) were purchased from Tianjin Fuchen Chemical Co., Ltd., China. $Mg(NO_3)_2{\cdot}6H_2O$ was provided by Xiya Chemical Technology Co., Ltd., China. Ammonia (28 wt% $NH_3$ in $H_2O$) was obtained from Sinopharm Chemical Reagent Co., Ltd. The model oils with chlorine content of 150 ppmw were prepared by dissolving 1-chlorooctane or 1,2-dichlorobenzene into dodecane.

### 2. Preparation of Various Adsorbents

$TiO_2$-U and $TiO_2$-A were prepared by the precipitation method because the precipitation method is widely used in the preparation of metal oxides with high surface areas, nano-sized crystallites and controllable surface chemical properties by adjusting the types and concentrations of precipitant, and hydrolysis temperature [27-29]. The commonly used precipitants, urea and ammonia [1], were used to investigate the influence of the precipitant on the dechlorination capacity of $TiO_2$. $TiO_2$-A was prepared according to the following procedure. 7.7 g of $TiCl_4$ was dissolved in deionized water with $Ti^{4+}$ molar concentration of 1 mol/L. 1 mol/L of ammonia was then added into the solution dropwise under vigorous stirring at 25 °C until the pH value of the solution reached 6. After aging for 0.5 h, the mixture was filtered, and the filter cake was washed with excessive deionized water until no $Cl^-$ ions were detected. The obtained precipitate was dried at 120 °C for 12 h and calcined at 400 °C for 4 h at a heating rate of 5 °C/min.

$TiO_2$-U, $CeO_2$ and a series of $Ti_{(1-x)}Ce_xO_2$ bimetallic oxides (x= 0.1, 0.3, 0.5, 0.7, 0.9) were prepared by urea gelation/co-precipitation method as reported in our previous work [25]. $TiCl_4$, $(NH_4)_2Ce(NO_3)_6$ and urea with the molar ratio of (1−x): x : 8 were dissolved in deionized water. The solution was heated to 95-100 °C and kept in this temperature range until the pH value of the solution reached 6.0. The mixture was filtered after aging for 0.5 h, and the filter cake was washed with deionized water until no $Cl^-$ ions were detected. The obtained precipitate was dried at 120 °C for 12 h and calcined at 400 °C for 4 h at a heating rate of 5 °C/min.

MgO was prepared following the same procedure as $TiO_2$-A described above. 8.6 g of $Mg(NO_3)_2{\cdot}6H_2O$ was dissolved in deionized water with $Mg^{2+}$ molar concentration of 1 mol/L. 1 mol/L of ammonia was then added into the solution dropwise under vigorous stirring at 25 °C until the pH value of the solution reached 10.86. After aging for 0.5 h, the mixture was filtered, and the filter cake was washed with excessive deionized water until no $Cl^-$ ions were detected. The obtained precipitate was dried at 120 °C for 12 h and calcined at 550 °C for 4 h at a heating rate of 5 °C/min. CaO was prepared by calcination of $CaCO_3$ at 900 °C for 4 h at a heating rate of 5 °C/min.

### 3. Adsorptive Dechlorination Experiments

Adsorptive dechlorination experiments were conducted in a 100 mL three-necked flask equipped with a reflux condenser to prevent oil vaporization. In a typical run, 24 g of hydrocarbon oil was added in the flask and then nitrogen was bubbled in at the flow rate of 20 mL/min to avoid the oxidation of oil. When the hydrocarbon oil was heated to the desired temperature under vigorous stirring in an oil bath, 0.2 g of the adsorbent was added in the flask. 0.8 mL of the suspension was sampled separately at the adsorption time of 15 min, 30 min, 1 h, 2 h and 3 h, and then filtrated by a 0.45 μm filter before analysis.

### 4. Regeneration of $Ti_{0.7}Ce_{0.3}O_2$

After the dechlorination experiment, the spent $Ti_{0.7}Ce_{0.3}O_2$ was filtered and washed separately with 10 mL of acetone and 10 mL of deionized water to remove the adsorbed organic and inorganic chemicals, respectively. The washed $Ti_{0.7}Ce_{0.3}O_2$ was then dried at 110 °C for 12 h and calcined at 400 °C for 4 h. The regenerated $Ti_{0.7}Ce_{0.3}O_2$ was then taken for decholorination experiment again. The dechlorination-regeneration experiment was run for four times, and the regenerated $Ti_{0.7}Ce_{0.3}O_2$ was labeled as $Ti_{0.7}Ce_{0.3}O_2$-R. To identify the possible product of 1-chlorooctane adsorbed on the adsorbent, the acetone and water eluents of the spent $Ti_{0.7}Ce_{0.3}O_2$ were collected for analysis.

### 5. Sample Analysis

5-1. Determination of the Chlorine Content of Treated Oils

The chlorine content of the hydrocarbon oils was determined by a TCS-300 Microcoulomb chlorine analyzer (Taizhou Tianchuang Instrument Co., China).

The chlorine removal of the model hydrocarbon oils was calculated by the following equation:

$$\varphi = \frac{C_0 - C_i}{C_0} \times 100\%$$

where $\varphi$ is the chlorine removal; $C_0$ and $C_i$ stand for the chlorine content (μg/g) of the initial model fuel and the treated model oil at different adsorption time, respectively.

5-2. Identification of the Products of 1-Chlorooctane

The acetone eluent of the spent $Ti_{0.7}Ce_{0.3}O_2$ was analyzed using a gas chromatogram (Agilent 7890B/5977A) equipped with a DB-5ms capillary column (60 m×0.25 mm×0.25 μm) and a mass spectrometer (GC-MS) to identify the organic products of 1-chlorooctane.

The water eluent of the spent $Ti_{0.7}Ce_{0.3}O_2$ was analyzed by a ion chromatogram (792 Basic IC, Metrohm) equipped with a Metrosep A SUPP 4 column to identify the chloride ion on the adsorbent.

**6. Characterization**

$N_2$ adsorption was conducted at 77 K using a Micromeritics ASAP2020 surface area and porosimetry analyzer. Textural properties of samples were determined by analyzing $N_2$ adsorption isotherms. The specific surface area was calculated using the BET equation in the $p/p_0$ range 0.05-0.2. The average pore size was evaluated using the BJH model. The total pore volume was estimated by the adsorbed $N_2$ at the relative pressure of 0.99.

XRD patterns of samples were collected using an XRD-7000 powder diffractometer (Shimadzu, Japan) with Cu K$\alpha$ radiation. The instrument was operated at a scanning rate of 1°/min in the 2$\theta$ range of 10-80° with the voltage of 40 kV and the current of 30 mA. The FT-IR spectra of samples were recorded on a Thermo Nicolet Nexus 410 spectrometer at a resolution of 4 $cm^{-1}$. The pyridine-IR analysis was conducted on a Nicolet 380 FTIR spectrometer. The IR spectra were recorded after desorption of pyridine under vacuum at 200 °C. $NH_3$-TPD and $CO_2$-TPD were carried out to measure the acidity and basicity of samples, respectively. The desorption signal of $NH_3$ or $CO_2$ was recorded with GAM200 mass spectrometry when the sample was heated from 100 °C to 700 °C at the temperature ramp of 10 °C/min. The desorbed $NH_3$ was absorbed by 0.025 mol/L of $H_2SO_4$ solution, followed by titration to calculate the acid amount of the sample, while the desorbed $CO_2$ was absorbed by 0.05 mol/L NaOH solution, followed by titration to calculate the base amount of the adsorbent.

## RESULTS AND DISCUSSION

**1. Influence of Precipitants on the Adsorptive Dechlorination Capacity of $TiO_2$**

Fig. 1 shows a comparison of dechlorination capacity of $TiO_2$-U and $TiO_2$-A prepared with urea and ammonia as the precipitants, respectively. It is evident that $TiO_2$-U showed higher dechlorination capacity than $TiO_2$-A, and the chlorine removal over $TiO_2$-U and $TiO_2$-A was 71.4% and 56.9% at the adsorption time of 3 h, respectively, indicating a significant influence of precipitants on the dechlorination capacity of $TiO_2$. The reason for the higher dechlorination capacity of $TiO_2$-U than $TiO_2$-A will be addressed in the characterization section.

**2. Influence of Ti/Ce Molar Ratio of $Ti_{(1-x)}Ce_xO_2$**

To improve the adsorptive dechlorination capacity of $TiO_2$-U,

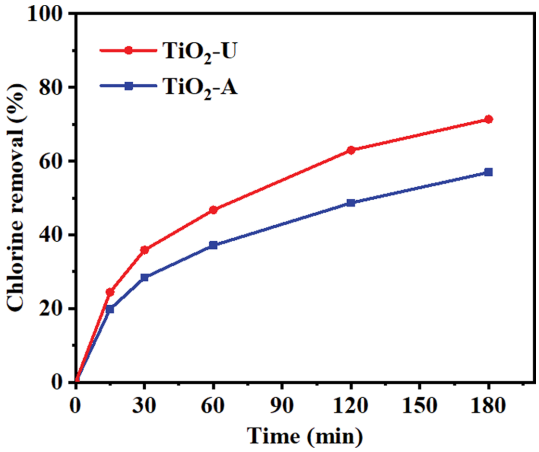


**Fig. 1. Dechlorination capacity of $TiO_2$-U and $TiO_2$-A.**

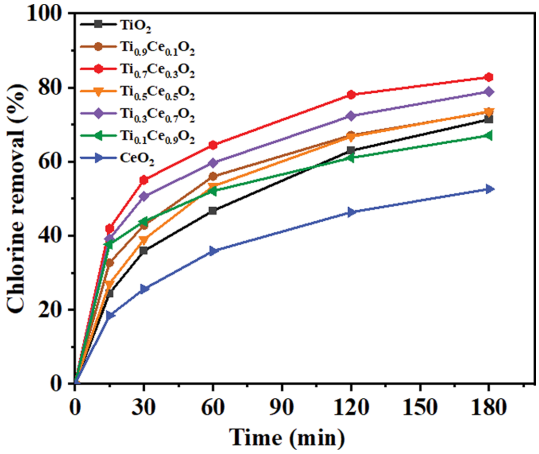


**Fig. 2. Comparison of dechlorination capacities of $Ti_{(1-x)}Ce_xO_2$ (x= 0, 0.1, 0.3, 0.5, 0.7, 0.9, 1).**

$CeO_2$ was incorporated into $TiO_2$-U, and the dechlorination capacity of $Ti_{(1-x)}Ce_xO_2$ bimetallic oxides with varying Ti/Ce molar ratio was evaluated. It can been seen from Fig. 2 that $Ti_{0.7}Ce_{0.3}O_2$ and $Ti_{0.3}Ce_{0.7}O_2$ exhibited significantly higher dechlorination capacity than $TiO_2$-U, and the chlorine removal over $Ti_{0.7}Ce_{0.3}O_2$ and $Ti_{0.3}Ce_{0.7}O_2$ reached 82.8% and 78.9%, respectively. $Ti_{0.9}Ce_{0.1}O_2$, $Ti_{0.5}Ce_{0.5}O_2$ and $Ti_{0.1}Ce_{0.9}O_2$ had very close dechlorination capacity to $TiO_2$-U, while the pure $CeO_2$ showed a much lower dechlorination capacity than $TiO_2$-U. The overall dechlorination capacity of various metal oxides followed the order of $Ti_{0.7}Ce_{0.3}O_2$>$Ti_{0.3}Ce_{0.7}O_2$>$Ti_{0.9}Ce_{0.1}O_2$≈ $Ti_{0.5}Ce_{0.5}O_2$≈$Ti_{0.1}Ce_{0.9}O_2$≈$TiO_2$-U>$CeO_2$. The reason for the difference in dechlorination capacity of various $Ti_{(1-x)}Ce_xO_2$ will be discussed in the characterization section.

**3. Promotion Effect of Alkaline Earth Metal Oxides**

To further improve the dechlorination capacity of $Ti_{0.7}Ce_{0.3}O_2$, 5 wt% of BaO, MgO and CaO, was separately mixed with $Ti_{0.7}Ce_{0.3}O_2$ and their dechlorination capacity for 1-chlorooctane was examined. As shown in Fig. 3, all the three composite metal oxides exhibited obviously higher dechlorination capacity than individual $Ti_{0.7}Ce_{0.3}O_2$ and alkaline earth metal oxides. The chlorine removal over $Ti_{0.7}Ce_{0.3}O_2$-BaO reached 92.1% at the adsorption time of 3 h,

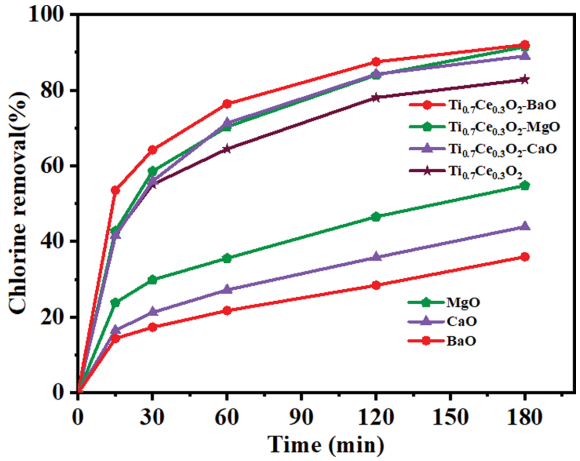


**Fig. 3. Dechlorination performance of the mixed oxides of $Ti_{0.7}Ce_{0.3}O_2$ with 5% of alkali metal oxides (MgO, CaO, BaO).**

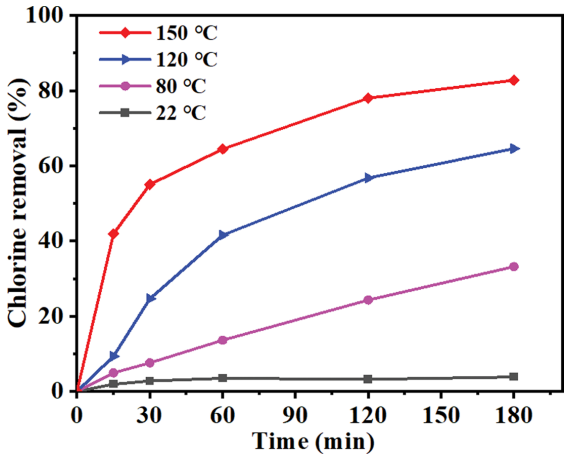


**Fig. 4. Adsorption of 1-chlorooctane over $Ti_{0.7}Ce_{0.3}O_2$ at different temperatures.**

which was higher than 72.54% over Zn/H$\beta$ [13], ~80% over Pd/Fe [30] and Ce-Y [18], but lower than 99% over $Al_2O_3$ reported in the literature. Considering the chlorine removal was obtained at different oil-to-adsorbent weight ratios, the adsorptive capacity of various adsorbents, which referred to the mass of chlorine removed by per unit mass of catalyst/adsorbent, was then calculated based on the data in literature and this work for comparison. From the data listed in Table 1, it can be seen that adsorptive dechlorination capacity over $Ti_{0.7}Ce_{0.3}O_2$-BaO reached 16.6 mg-Cl·g$^{-1}$, much higher than 1.98 mg-Cl·g$^{-1}$ over $Al_2O_3$, 1.2 mg-Cl·g$^{-1}$ over Zn/H$\beta$ and 8 mg-Cl·g$^{-1}$ over Pd/Fe, demonstrating superior dechlorination performance of $Ti_{0.7}Ce_{0.3}O_2$-BaO. The reason for the promotion effect of alkaline earth metal oxides will be discussed in the characterization section.

## 4. Influence of Adsorption Temperature

Fig. 4 presents the adsorption capacity of $Ti_{0.7}Ce_{0.3}O_2$ for 1-chlorooctane at different temperatures. It can be observed that $Ti_{0.7}Ce_{0.3}O_2$ exhibited poor adsorption capacity at 20 °C, and the chlorine removal was only 3.8% at the adsorption time of 3 h. As the temperature increased from 20 °C to 150 °C, the chlorine removal remarkably increased up to 82.8%, indicating that an increase of temperature had a positive effect on the adsorption capacity. It is well known that physical adsorption is exothermic, and increasing adsorption temperature will invariably lead to a decrease of uptake [31]. Therefore, we hypothesized that chemical transformation of 1-chlorooctane might occur on the adsorbent at elevated temperatures. From the results that 82.8% of chloride disappeared from the oil at the adsorption time of 3 h in the presence of $Ti_{0.7}Ce_{0.3}O_2$ at 150 °C, it was deduced that the product of the disappeared 1-chlorooctane was adsorbed on the $Ti_{0.7}Ce_{0.3}O_2$. The acetone eluent and the water eluent of the spent $Ti_{0.7}Ce_{0.3}O_2$ were then analyzed by GC-MS and IC, respectively.

Fig. 5 presents the gas chromatogram of the acetone eluent of the spent $Ti_{0.7}Ce_{0.3}O_2$. It is clear that besides dodecane and trace amounts of tridecane and tetradecane which were from the original oil, 1-octanol was detected at the retention time of 25.9 min, which was identified by comparing its mass spectrum with the standard mass spectrum of 1-octanol (Fig. 6(a)). This result indicated 1-chlorooctane was converted to 1-octanol over the adsorbent at elevated temperature. It is worth noting that during the adsorption process, nitrogen was bubbled and air was absent from the adsorption system, so it can be inferred that the hydroxyl group in 1-octanol did not originate from the oxidation of 1-chlorooctane by air but the oxygen-containing species on the adsorbent. Fig. 6(b) shows the ion chromatograms of ultrapure water, eluents of fresh $Ti_{0.7}Ce_{0.3}O_2$, and the spent $Ti_{0.7}Ce_{0.3}O_2$. It is observed only trace amount of $Cl^-$ was detected in ultrapure water and the eluent of fresh $Ti_{0.7}Ce_{0.3}O_2$. In a sharp contrast, a huge increase of $Cl^-$ in the eluent of the spent $Ti_{0.7}Ce_{0.3}O_2$ was observed, implying large amounts of $Cl^-$ were generated on the adsorbent.

**Table 1. Comparison of dechlorination performance of $Ti_{0.7}Ce_{0.3}O_2$-BaO and different adsorbents reported in the literature**

| Adsorbents | Initial chlorine content (ppmw) | The weight ratio of oil to adsorbent | Adsorption temperature (°C) | Chlorine removal (%) | Adsorption capacity (mg-Cl/g) |
|---|---|---|---|---|---|
| Zn/H$\beta$ [13] | 60 | 28 : 1 | 25 | 72.54 | 1.2 |
| Pd/Fe [30] | 100 | 100 : 1 | 22 | ~80 | 8 |
| $Al_2O_3$ [1] | 50 | 40 : 1 | 150 | 99 | 1.98 |
| Ce-Y [18] | 50 | Dynamic test, LHSV : 10 h$^{-1}$ | 150 | ~80 | |
| $Ti_{0.7}Ce_{0.3}O_2$-BaO (used in this work) | 150 | 120 : 1 | 150 °C | 92.1 | 16.6 |

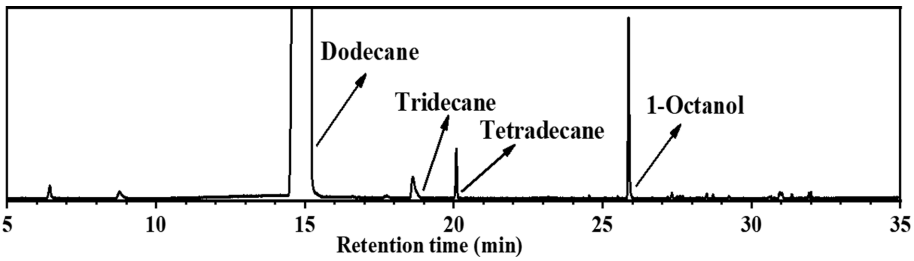


**Fig. 5. Gas chromatogram of the acetone eluent of the spent $Ti_{0.7}Ce_{0.3}O_2$.**

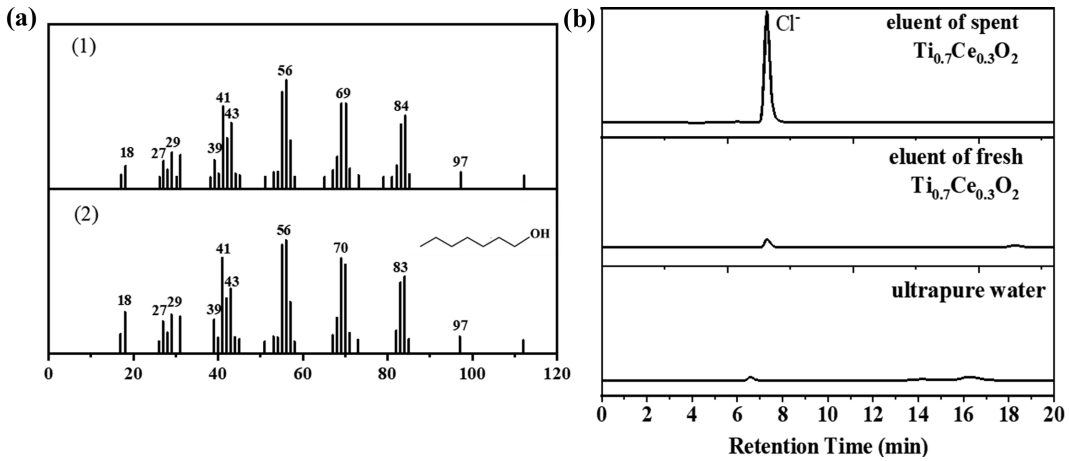


**Fig. 6. (a) Mass spectra of the substance at the retention time of 25.9 min (1) and standard mass spectrum of 1-octanol (2). (b) Ion chromatograms of ultrapure water, eluents of fresh $Ti_{0.7}Ce_{0.3}O_2$ and spent $Ti_{0.7}Ce_{0.3}O_2$.**

The above results demonstrate that 1-chlorooctane in the model oil was converted to $Cl^-$ and 1-octanol on the adsorbent at 150 °C, which were then adsorbed, implying the mechanism of reactive adsorption dechlorination.

**5. Regeneration of $Ti_{0.7}Ce_{0.3}O_2$**

Fig. 7 shows the recycling performance of $Ti_{0.7}Ce_{0.3}O_2$ in a series of four consecutive dechlorination-regeneration cycles. It is clear that after the first regeneration, the dechlorination capacity of $Ti_{0.7}Ce_{0.3}O_2$ for 1-chlorooctane slightly decreased. However, the dechlorination capacity of $Ti_{0.7}Ce_{0.3}O_2$ remained basically stable in the following dechlorination-regeneration cycles, and chlorine removal still retained 71.4% in the fourth regeneration cycle, implying good regenerability of $Ti_{0.7}Ce_{0.3}O_2$. The reason for the slight decrease of dechlorination performance of $Ti_{0.7}Ce_{0.3}O_2$ after four consecutive dechlorination-regeneration cycles will be addressed in the characterization section.

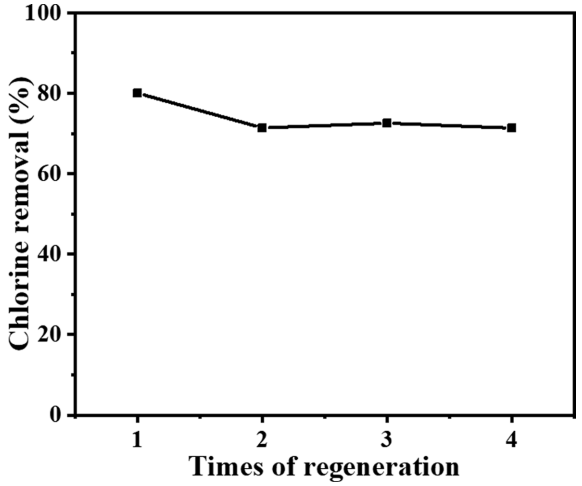


**Fig. 7. Regeneration cycles of $Ti_{0.7}Ce_{0.3}O_2$.**

**6. Characterization**

Fig. 8 gives the XRD patterns of various metal oxides. It can be seen from Fig. 8(a) that both $TiO_2$-U and $TiO_2$-A show clear diffraction peaks at $2\theta$=25.28°, 37.80°, 48.05°, 53.89°, 55.06°, 62.88°, which correspond to reflections of anatase phase (101), (004), (200), (105), (211), (213) planes (JCPDS No. 84-1286), indicating both $TiO_2$-U and $TiO_2$-A were present in the anatase phase. Nevertheless, $TiO_2$-U precipitated by urea shows slightly weaker diffraction peak at $2\theta$=25.28° than $TiO_2$-A precipitated by ammonia, indicating the smaller crystalline size of the former, which was due to slower hydrolysis rate in case of urea [32]. $CeO_2$ shows characteristic peaks of fluorite phase at $2\theta$=28.6°, 33.2°, 47.7° and 56.6° (JCPDS NO.43-1002). Compared to $TiO_2$-U and $CeO_2$ single metal oxides, various $Ti_{(1-x)}Ce_xO_2$ bimetallic oxides show weaker characteristic peaks of anatase $TiO_2$ or fluorite $CeO_2$, implying the decrease of the crystalline sizes, which was attributed to the dissimilar nuclei, coordination geometry and inhibition of individual crystallization [33]. From Fig. 8(b), it is observed that in comparison to fresh $Ti_{0.7}Ce_{0.3}O_2$, $Ti_{0.7}Ce_{0.3}O_2$-R shows a slightly decreased diffraction peak at $2\theta$=25.28°, suggesting some loss of crystallinity.

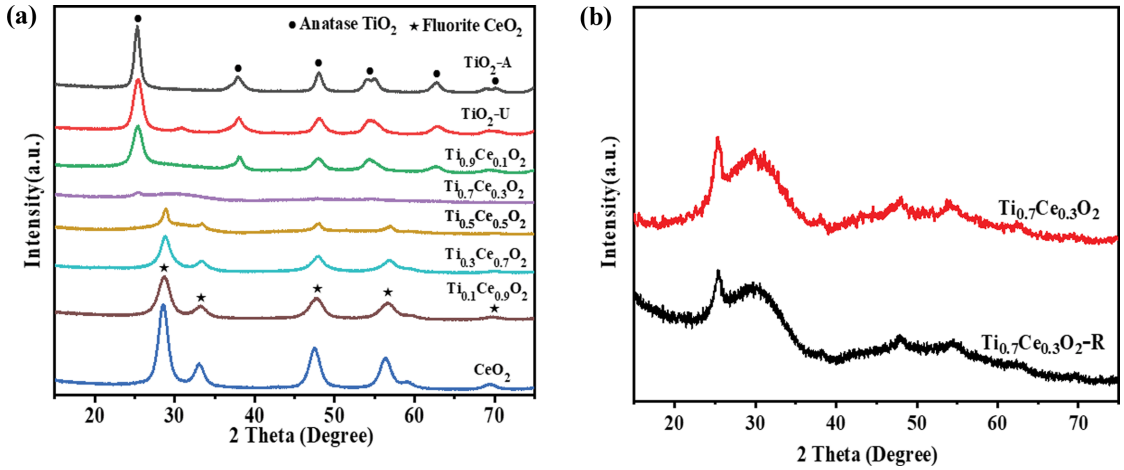


**Fig. 8. (a) XRD patterns of various metal oxides. (b) XRD patterns of $Ti_{0.7}Ce_{0.3}O_2$ and the regenerated $Ti_{0.7}Ce_{0.3}O_2$-R.**

**Table 2. Textural properties of various adsorbents**

| Adsorbents | BET surface area ($m^2$/g) | Total pore volume ($cm^3$/g) | Average pore size (nm) |
|---|---|---|---|
| $TiO_2$-A | 121.3 | 0.2050 | 6.60 |
| $TiO_2$-U | 152.3 | 0.3288 | 8.51 |
| $Ti_{0.9}Ce_{0.1}O_2$ | 158.8 | 0.5648 | 14.13 |
| $Ti_{0.7}Ce_{0.3}O_2$ | 174.9 | 0.6017 | 14.19 |
| $Ti_{0.7}Ce_{0.3}O_2$-R | 155.5 | 0.2964 | 7.49 |
| $Ti_{0.5}Ce_{0.5}O_2$ | 211.1 | 0.2649 | 4.80 |
| $Ti_{0.3}Ce_{0.7}O_2$ | 191.0 | 0.2599 | 5.22 |
| $Ti_{0.1}Ce_{0.9}O_2$ | 199.7 | 0.2258 | 4.22 |
| $CeO_2$ | 142.2 | 0.1301 | 3.22 |

Table 2 lists the textural properties of various metal oxides. As shown, various metal oxides possess mesoporous structure with average pore size range of 4-15 nm, which is beneficial for the diffusion and adsorption of organochlorine compounds. For $TiO_2$ prepared with different precipitants, $TiO_2$-U exhibits larger surface area than $TiO_2$-A, which was attributed to smaller crystalline size of the former, as characterized by XRD analysis. Compared to $TiO_2$-U and $CeO_2$ single oxides, various $Ti_{(1-x)}Ce_xO_2$ bimetallic oxides show obviously increased surface areas also due to the decrease of the crystalline sizes. Surprisingly, $Ti_{0.7}Ce_{0.3}O_2$, which exhibits the highest dechlorination capacity, did not have the highest surface area, suggesting that the surface area was not the dominant factor affecting dechlorination capacity of various metal oxides. In comparison to fresh $Ti_{0.7}Ce_{0.3}O_2$, the regenerated $Ti_{0.7}Ce_{0.3}O_2$-R had the decreased surface area and pore volume, implying the collapse or blockage of some pores after four dechlorination-regeneration cycles, which might be one factor that led to the decrease of its dechlorination capacity.

FT-IR was carried out to determine the surface oxygen-containing species on various metal oxides. Fig. 9(a) illustrates FT-IR spectra of $TiO_2$-A, $TiO_2$-U, $CeO_2$ and a representative bimetallic oxide $Ti_{0.7}Ce_{0.3}O_2$. It can be seen that all the four metal oxides show evident absorption bands at around 3,426 $cm^{-1}$ (diffuse band) and 1,627 $cm^{-1}$ (weak band), corresponding to the stretching vibrations of -OH groups and the bending vibrations of $H_2O$ molecules, respectively [34-37]. The appearance of these bands implies the presence of -OH groups and $H_2O$ molecules on the surface of the four metal oxides. Fig. 9(b) reveals that compared to the fresh $Ti_{0.7}Ce_{0.3}O_2$, the regenerated $Ti_{0.7}Ce_{0.3}O_2$ shows slightly decreased absorption bands

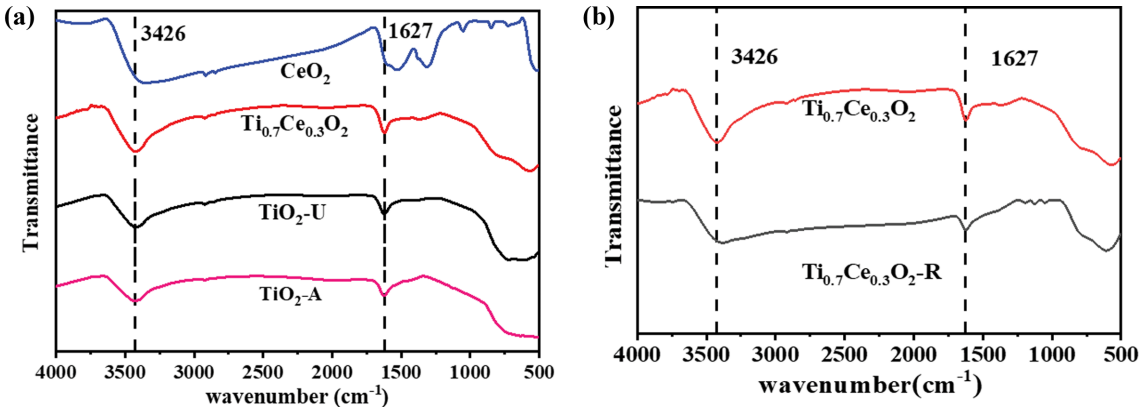


**Fig. 9. (a) FT-IR spectra of $TiO_2$-A, $TiO_2$-U, $Ti_{0.7}Ce_{0.3}O_2$ and $CeO_2$. (b) FT-IR spectra of $Ti_{0.7}Ce_{0.3}O_2$ and $Ti_{0.7}Ce_{0.3}O_2$-R.**

at 3,426 $cm^{-1}$ and 1,627 $cm^{-1}$, indicating the reduction of -OH groups and adsorbed water after recycling tests.

It was reported that organochlorine compounds would be hydrolyzed to HCl and oxygen-containing compounds in the presence of alkalis or a solid catalyst [11,38-40]. Lu [40] reported that 95% of the chlorine in PVC was effectively converted to HCl by hydrolysis process within 2 h at 240 °C, and -OH groups were attached onto the residual plastic. Khaleel [11] conducted catalytic dechlorination of $CCl_4$ over $Al_2O_3$ in the presence of trace amount of water, and found that $CCl_4$ was hydrolyzed to form $CO_2$ and HCl, and the conversion of $CCl_4$ reached 100% in the presence of trace amount of water, much higher than 5% in the absent of water. Similarly, based on the analysis result in this work that 1-chlorooctane was converted to 1-octanol and $Cl^-$, it can be speculated that in the presence of $H_2O$ on $TiO_2$-based metal oxides, 1-chlorooctane might undergo catalytic hydrolysis to generate 1-octanol and HCl at 150 °C.

Pyridine-IR was conducted to determine the type of acidic sites on $TiO_2$-U, $CeO_2$ and the representative bimetallic oxides $Ti_{0.7}Ce_{0.3}O_2$. Generally speaking, ν(C-C) vibration of pyridine adsorbed on Lewis acidic sites exhibits an absorption band at around 1,450 $cm^{-1}$, while the vibration of pyridine adsorbed on Brønsted acidic sites shows an absorption band at around 1,540 $cm^{-1}$ [41]. As shown in Fig. 10, an obvious absorption band at around 1,446 $cm^{-1}$ is observed in the wavenumber range of 1,400-1,600 $cm^{-1}$ over each of the three oxides, indicating the existence of Lewis acidic sites on the metal oxides. However, no clear absorption band at around 1,540 $cm^{-1}$ is observed on all these metals oxides, implying the absence of Brønsted acidic sites on them.

The above Pyridine-IR analysis demonstrates that various metal oxides have only Lewis acidic sites. To further analyze the strength of Lewis acid on various metal oxides, $NH_3$-TPD was carried out. Fig. 11 exhibits $NH_3$-TPD profiles of various metal oxides. Normally, the peaks in the temperature ranges of 100-200 °C, 200-400 °C and over 400 °C represent $NH_3$ desorption from weak acidic sites, moderately strong acidic sites and strong acidic sites on the adsorbents, respectively [18]. It can be observed from Fig. 11(a) the $NH_3$ desorption peak over $TiO_2$-A located in the temperature range of 200-700 °C, implying the existence of moderately strong acidic sites and strong acidic sites on $TiO_2$-A. Different from $TiO_2$-A, $TiO_2$-U exhibits a $NH_3$ desorption peak in the temperature range of 100-600 °C, indicating the presence of Lewis acidic sites of three different strengths. Similarly, $CeO_2$ and all of the $Ti_{(1-x)}Ce_xO_2$ bimetallic oxides show broad $NH_3$ desorption peaks, but the peaks mostly located in the temperature range of 200-400 °C, implying $CeO_2$ and the bimetallic oxides contain mainly moderately strong Lewis acidic sites. It is clear in Fig. 11(b) that the peak temperature of $NH_3$ desorption was shifted from 298 °C for fresh $Ti_{0.7}Ce_{0.3}O_2$ to 242 °C for the regenerated $Ti_{0.7}Ce_{0.3}O_2$, indicating loss of some moderately strong Lewis acidic sites after recycling tests.

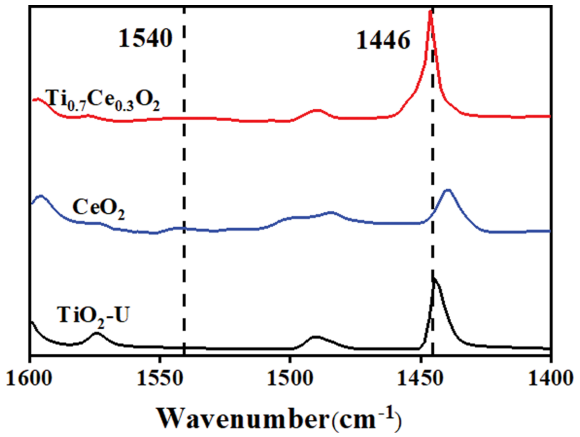


**Fig. 10. Pyridine-IR patterns of $TiO_2$-U, $CeO_2$ and $Ti_{0.7}Ce_{0.3}O_2$ after desorption at 200 °C.**

To investigate the influence of acid amount of the adsorbent on the dechlorination capacity, the amounts of acidic sites on various metal oxides were determined by absorption of outlet gas with 0.025 mol/L of $H_2SO_4$ solution followed by titration, and the data

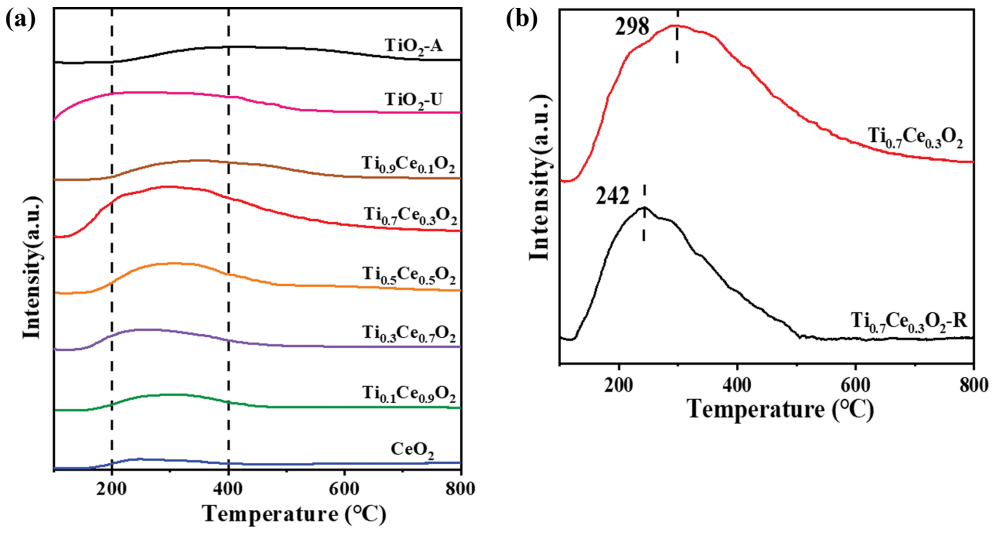


**Fig. 11. (a) $NH_3$-TPD profiles of various metal oxides. (b) $NH_3$-TPD profiles of $Ti_{0.7}Ce_{0.3}O_2$ and the regenerated $Ti_{0.7}Ce_{0.3}O_2$-R.**

**Table 3. Total acid amounts of various metal oxides**

| Materials | Total acid amount (mmol/g) | Materials | Total acid amount (mmol/g) |
|---|---|---|---|
| $TiO_2$-A | 0.4808 | $Ti_{0.5}Ce_{0.5}O_2$ | 0.5690 |
| $TiO_2$-U | 0.7216 | $Ti_{0.3}Ce_{0.7}O_2$ | 0.4510 |
| $Ti_{0.9}Ce_{0.1}O_2$ | 0.5470 | $Ti_{0.1}Ce_{0.9}O_2$ | 0.4300 |
| $Ti_{0.7}Ce_{0.3}O_2$ | 0.8263 | $CeO_2$ | 0.1005 |
| $Ti_{0.7}Ce_{0.3}O_2$-R | 0.6203 | | |

is listed in Table 3. It shows that $TiO_2$-U had a greater acid amount than $TiO_2$-A. Interestingly, $TiO_2$-U also exhibited higher dechlorination capacity than $TiO_2$-A (Fig. 1). This consistency suggests the acid amount of the adsorbent might play an important role in its dechlorination capacity. Among various $Ti_{(1-x)}Ce_xO_2$ bimetallic oxides and the single oxides, $Ti_{0.7}Ce_{0.3}O_2$ had the most acid amount and also the highest dechlorination capacity, while $CeO_2$ had the least acid amount and also the lowest dechlorination capacity. Moreover, $Ti_{0.3}Ce_{0.7}O_2$-R had less acid amount and also showed lower dechlorination capacity than fresh $Ti_{0.3}Ce_{0.7}O_2$. These results confirm the significant role of acid amount of the adsorbent on its dechlorination capacity. Zhang [13] and Lee [42] also reported the acidity of a adsorbent or catalyst played a significant role in its dechlorination performance. Similarly, in Friedel-Crafts alkylation reaction, a Lewis acid catalyst, i.e. $AlCl_3$, was usually used to activate C-Cl bond in chlorinated hydrocarbon [43]. Therefore, it can be speculated that in the reactive adsorption process of organochlorine over $TiO_2$-based metal oxides, the Lewis acid acted as the sites for the adsorption and activation of C-Cl bond.

However, it was also observed that $Ti_{0.3}Ce_{0.7}O_2$ had less acid amount but higher dechlorination capacity than $TiO_2$-U (Table 3 and Fig. 2), implying that besides the acidity, some other physical and chemical properties of the adsorbent may also play an important role on its dechlorination capacity, e.g., surface area, basicity, etc. The higher surface area of $Ti_{0.3}Ce_{0.7}O_2$ (Table 2) may be one factor that led to its higher dechlorination capacity than $TiO_2$-U.

$CO_2$-TPD was conducted to investigate the influence of the basicity of metal oxide on its dechlorination capacity, and the $CO_2$-TPD profiles of various metal oxides are illustrated in Fig. 12. Usually, the desorption peaks of $CO_2$ in the temperature ranges of 100-300 °C, 300-500 °C and over 500 °C are ascribed to $CO_2$ desorption from weak basic sites, moderately strong basic sites and strong basic sites, respectively [44]. It can be observed from Fig. 12(a) that both $TiO_2$-A and $TiO_2$-U exhibit two desorption peaks separately in the temperature ranges of 100-300 °C and over 500 °C, indicating the presence of weak and strong basic sites on them. A broad desorption peak in the range of 200-600 °C is observed over $CeO_2$, implying the presence of basic sites of three different strengths. Various $Ti_{(1-x)}Ce_xO_2$ bimetallic oxides exhibit quite different $CO_2$ desorption behavior, indicating the significant impact of Ti/Ce molar ratio on the basicity of $Ti_{(1-x)}Ce_xO_2$. Fig. 12(b) reveals that after recycling tests, the peak below 300 °C corresponding to $CO_2$ desorption from weak basic sites on $Ti_{0.7}Ce_{0.3}O_2$ disappeared, while a small peak in the temperature range of 300-500 °C appeared, which was corresponding to $CO_2$ desorption from moderately strong basic sites. The remarkable change of basicity of $Ti_{0.7}Ce_{0.3}O_2$ after recycling tests implies the basic sites of $Ti_{0.7}Ce_{0.3}O_2$ might participate in the reactive adsorption dechlorination of organochlorine compounds.

To investigate the influence of base amounts of the metal oxides on their dechlorination capacity, the amounts of basic sites on various metal oxides were determined by absorption of outlet gas with 0.05 mol/L of NaOH solution followed by titration. The data listed in Table 4 shows that $TiO_2$-A and $TiO_2$-U had comparable base amounts. Among various $Ti_{(1-x)}Ce_xO_2$ bimetallic oxides and the single oxides, $Ti_{0.7}Ce_{0.3}O_2$ with the highest dechlorination capacity,

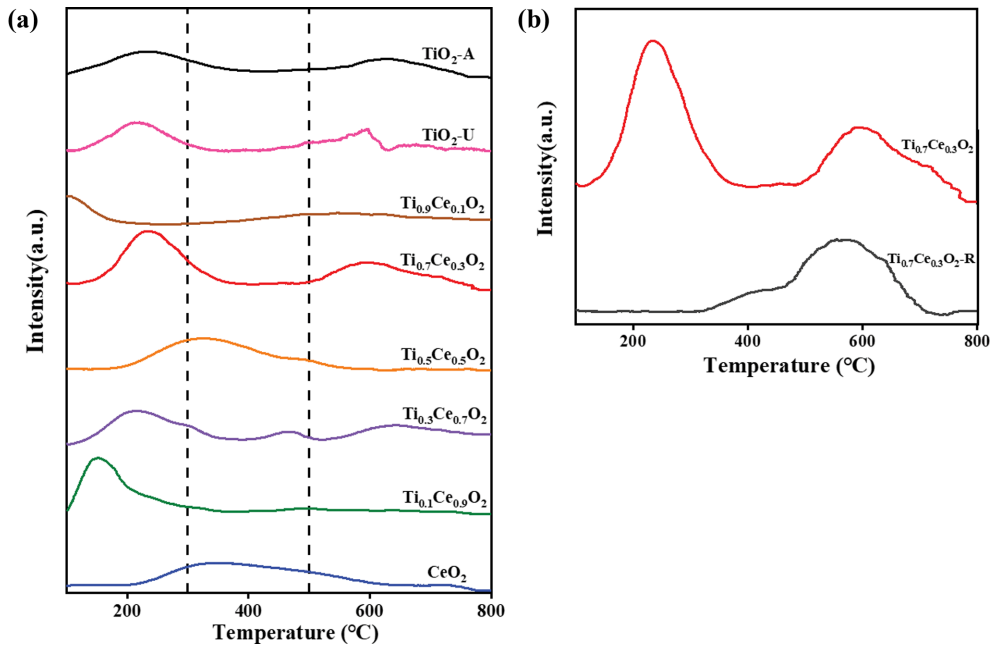


**Fig. 12. (a) $CO_2$-TPD profiles of various metal oxides. (b) $CO_2$-TPD profiles of $Ti_{0.7}Ce_{0.3}O_2$ and the regenerated $Ti_{0.7}Ce_{0.3}O_2$-R.**

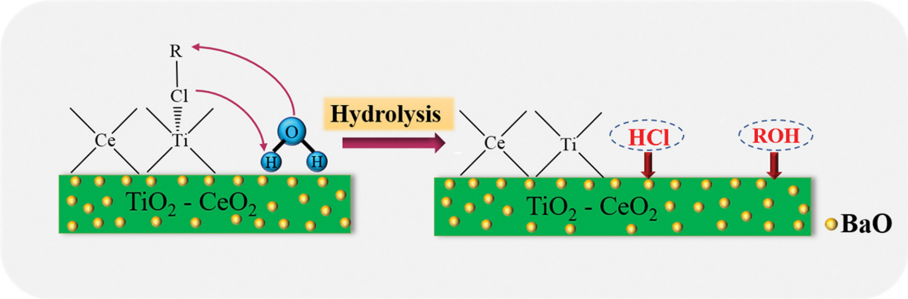


**Fig. 13. Scheme of the mechanism of reactive adsorption dechlorination of hydrocarbon oil over $Ti_{0.7}Ce_{0.3}O_2$-BaO.**

**Table 4. Total base amounts of various metal oxides**

| Materials | Total base amount (mmol/g) | Materials | Total base amount (mmol/g) |
|---|---|---|---|
| $TiO_2$-A | 0.0645 | $Ti_{0.5}Ce_{0.5}O_2$ | 0.0678 |
| $TiO_2$-U | 0.0637 | $Ti_{0.3}Ce_{0.7}O_2$ | 0.0745 |
| $Ti_{0.9}Ce_{0.1}O_2$ | 0.0730 | $Ti_{0.1}Ce_{0.9}O_2$ | 0.0503 |
| $Ti_{0.7}Ce_{0.3}O_2$ | 0.1125 | $CeO_2$ | 0.0624 |
| $Ti_{0.7}Ce_{0.3}O_2$-R | 0.0507 | | |

also had the most base amounts. Moreover, $Ti_{0.3}Ce_{0.7}O_2$ had more base amount than $TiO_2$-U, which could be another reason that led to its higher dechlorination capacity than $TiO_2$-U. Compared with the fresh $Ti_{0.7}Ce_{0.3}O_2$, $Ti_{0.7}Ce_{0.3}O_2$-R, which showed lower dechlorination capacity, also had dramatically less base amount. Moreover, mixing 5 wt% of alkali earth metal oxide into $Ti_{0.7}Ce_{0.3}O_2$ mechanically enhanced its dechlorination capacity. These results strongly suggest the significant impact of base amount on the dechlorination capacity of the metal oxide. The basic sites on the adsorbent may act as the sites for adsorption of the generated HCl to avoid the poisoning of Lewis acid sites because it was reported that HCl could seriously deactivate the catalyst for dechlorination [12, 45].

**7. Possible Mechanism**

Based on the above results and discussions, the mechanism of reactive adsorption dechlorination over $TiO_2$-based metal oxides can be proposed, and the scheme is illustrated in Fig. 13. Organochlorine was activated on the Lewis acid sites of $TiO_2$-based metal oxide at elevated temperatures, and then hydrolyzed to form ROH and HCl in the presence of trace amount of $H_2O$ molecules on the metal oxides. The generated HCl was adsorbed on the basic sites, and ROH was also adsorbed on the surface of $TiO_2$-based metal oxides.

## CONCLUSION

This work addresses reactive adsorption dechlorination of hydrocarbon oil over $TiO_2$-based metal oxides. $TiO_2$-U precipitated by urea exhibited higher dechlorination capacity than $TiO_2$-A precipitated by ammonia. Among various $Ti_{(1-x)}Ce_xO_2$ bimetallic oxides, $Ti_{0.7}Ce_{0.3}O_2$ showed the highest dechlorination capacity, and the chlorine removal over $Ti_{0.7}Ce_{0.3}O_2$ reached 82.8% after adsorption at 150 °C for 3 h. The chlorine removal was further increased to 92.1% when mechanically mixing 5 wt% of BaO into $Ti_{0.7}Ce_{0.3}O_2$. Both the acidity and basicity of the adsorbent played an important role in its dechlorination capacity. The removal of organochlorine over $TiO_2$-based metal oxides followed the mechanism of reactive adsorption. Organochlorine was hydrolyzed to form ROH and HCl in the presence of trace amount of $H_2O$ molecules on the Lewis acid sites of $TiO_2$-based metal oxide at elevated temperatures, which were then adsorbed on the basic sites of the adsorbent. Our findings provide a new insight for deep dechlorination of hydrocarbon oil, and future work should focus on the development of adsorbents with large Lewis acid and base amount of strong strength, as well as high surface area.

## ACKNOWLEDGEMENTS

This work was supported by the National Natural Science Foundation of China (No. 21905027), Beijing Education Committee Science and Technology Project (KM202010017007), and the Innovation and Entrepreneurship Training Program for College Students (No. 2021J00084).

## NOTES

The authors declare that there are no known competing financial interests or personal relationships that could influence the work reported in this paper.

## REFERENCES

1. H. Niu, D. Zhao, G. Xie, Y. Yuan, W. Zhang, C. Zhang, C. Li and L. Cui, *Fuel*, **304**, 121410 (2021).
2. X. L. Ge, L. Shi and X. Wang, *Ind. Eng. Chem. Res.*, **53**, 6351 (2014).
3. G. Z. Jiang, D. A. S. Monsalve, P. Clough, Y. Jiang and G. A. Leeke, *Acs Sustain. Chem. Eng.*, **9**, 1576 (2021).
4. B. Wu, Y. Li, X. Li and J. Zhu, *Energy Fuels*, **29**, 1391 (2015).
5. L. Xu, E. E. Stangland, J. A. Dumesic and M. Mavrikakis, *Acs Catal.*, **11**, 7890 (2021).
6. P. Zhao, N. Huang, J. Li and X. Cui, *Fuel Process. Technol.*, **199**, 106277 (2020).
7. V. K. Soni, G. Singh, B. K. Vijayan, A. Chopra, G. S. Kapur and S. S. V. Ramakumar, *Energy Fuels*, **35**, 12763 (2021).
8. R. Palos, A. Gutiérrez, F. J. Vela, M. Olazar, J. M. Arandes and J. Bilbao, *Energy Fuels*, **35**, 3529 (2021).

9. M. R. Ball, K. R. Rivera-Dones, E. Stangland, M. Mavrikakis and J. A. Dumesic, *J. Catal.*, **370**, 241 (2019).
10. J. Sun, Y. Han, H. Fu, H. Wan, Z. Xu and S. Zheng, *Appl. Surf. Sci.*, **428**, 703 (2018).
11. A. Khaleel, *Micropor. Mesopor. Mater.*, **91**, 53 (2006).
12. N. Lingaiah, M. A. Uddin, A. Muto, Y. Sakata and K. Murata, *Appl. Catal. A Gen.*, **207**, 79 (2001).
13. N. Zhang, R. Li, G. Zhang, L. Dong and T. J. A. O. Li, *Acs Omega*, **5**, 11987 (2020).
14. J. Chen, X. Zhao and Z. Ying, *China Pet. Process Pe.*, **19**, 23 (2017).
15. Y. Mu, G. Zhan, C. Huang, X. Wang, Z. Ai, J. Zou, S. Luo and L. Zhang, *Environ. Sci. Technol.*, **53**, 3208 (2019).
16. V. Najafi, E. Ahmadi and F. Ziaee, *Iran. Polym. J.*, **27**, 841 (2018).
17. S. R. Lee, J. M. Cho, M. Son, M. J. Park, W. Y. Kim, S. Y. Kim and J. W. Bae, *Chem. Eng. J.*, **331**, 56 (2018).
18. X. Ge, L. Shi and X. Wang, *Ind. Eng. Chem. Res.*, **53**, 6351 (2014).
19. M. . Uddin, A. Muto, T. Imai and Y. Sakata, *Fuel*, **80**, 1901 (2001).
20. G. Jiang, D. Monsalve, P. Clough, Y. Jiang and G. A. Leeke, *ACS Sustain. Chem. Eng.*, **9**, 1576 (2021).
21. A. Lopez-Urionabarrenechea, I. de Marco, B. M. Caballero, M. F. Laresgoiti and A. Adrados, *Fuel Process. Technol.*, **137**, 229 (2015).
22. W. Zhu, Y. Xu, H. Li, B. Dai, H. Xu, C. Wang, Y. Chao and H. Liu, *Korean J. Chem. Eng.*, **31**, 211 (2014).
23. S. S. Chen, H. C. Hsi, S. H. Nian and C. H. Chiu, *Appl. Catal. B*, **160**, 558 (2014).
24. J. Guo, S. Watanabe, M. J. Janik, X. Ma and C. Song, *Catal. Today*, **149**, 218 (2010).
25. W. Zhang, X. Li, H. Wang, Y. Song, S. Zhang and C. Li, *Korean J. Chem. Eng.*, **34**, 3132 (2017).
26. J. Xiao, S. Sitamraju, Y. Chen, S. Watanabe, M. Fujii, M. Janik and C. Song, *AIChE J.*, **61**, 631 (2015).
27. X. C. Xiao, B. G. Peng, L. F. Cai, X. M. Zhang, S. R. Liu and Y. D. Wang, *Sci. Rep.*, **8**, 7571 (2018).
28. Y. J. Wang, J. M. Ma, M. F. Luo, P. Fang and M. He, *J. Rare Earth*, **25**, 58 (2007).
29. W. Zhang, X. Li, H. Wang, Y. J. Song, S. H. Zhang and C. Q. Li, *Korean J. Chem. Eng.*, **34**, 3132 (2017).
30. X. Wang, C. Chen, Y. Chang and H. Liu, *J. Hazard. Mater.*, **161**, 815 (2009).
31. H. Zhen, X. Qian, Y. Hu and J. Cheng, *Chem. Eng. J.*, **209**, 547 (2012).
32. S. Watanabe, *J. Phy. Chem. C*, **113**, 14249 (2009).
33. M. Dahl, Y. Liu and Y. Yin, *Chem. Rev.*, **114**, 9853 (2014).
34. A. Adamczyk and E. Długon, *Spectrochim. Acta A Mol. Biomol. Spectrosc.*, **89**, 11 (2012).
35. M. D. Hernández-Alonso, I. Tejedor-Tejedor, J. M. Coronado, M. A. Anderson and J. Soria, *Catal. Today*, **143**, 364 (2009).
36. M. Xie, L. Jing, Z. Jia, J. Lin and H. Fu, *J. Hazard. Mater.*, **176**, 139 (2010).
37. P. Parthasarathy and S. Vivekanandan, *Ain Shams Eng. J.*, **11**, 777 (2020).
38. Z. Sun, F. Takahashi, O. Yu, K. Fukushi, Y. Oshima and K. Yamamoto, *Chemosphere*, **66**, 151 (2007).
39. J. Lu, S. Ma, J. Gao, J. Freitas and T. J. Bonagamba, *J. Appl. Polym. Sci.*, **90**, 3252 (2010).
40. J. Lu, S. Ma and J. Gao, *Energy Fuels*, **16**, 1251 (2002).
41. H. Song, H. Gao, H. Song, G. Yang and X. Li, *Ind. Eng. Chem. Res.*, **55**, 3813 (2016).
42. C. Lee, Y. Jin, J. Kim, S. H. Park, B. H. Chun and S. H. Kim, *J. Ind. Eng. Chem.*, **19**, 1443 (2013).
43. Y. Zhou, X. Y. Li, S. L. Hou and J. X. Xu, *J. Mol. Catal. A: Chem.*, **365**, 203 (2012).
44. S. Li, G. Liu, S. Zhang, K. An and Z. Ma, *J. Energy Chem.*, **43**, 167 (2020).
45. N. Lingaiah, M. A. Uddin, K. Morikawa, A. Muto, Y. Sakata and K. Murata, *Green Chem.*, **3**, 74 (2001).